Inorganic Chemistry

Article

pubs.acs.org/IC

$CsCoO_2$ Featuring a Novel Polyoxocobaltate(III) Anion Based on a Two-Dimensional Architecture of Interconnected Tetrahedra

Naveed Zafar Ali, Jürgen Nuss, Reinhard K. Kremer, and Martin Jansen*

Max Planck Institute for Solid State Research, Heisenbergstr.1, 70569 Stuttgart, Germany

Supporting Information

ABSTRACT: $CsCoO_2$ has been prepared along the azide/nitrate route as a reddish black microcrystalline powder at 833 K. According to single crystal X-ray analysis, the title compound crystallizes as a structure type novel for oxides (*Cmca*, $Z = 8$, $a = 5.9841(1)$ Å, $b = 12.2458(2)$ Å, $c = 8.2650(1)$ Å). The prominent features of the structure are pairs of edge-linked CoO_4 tetrahedra to form Co_2O_6 dimers, which are condensed by vertex sharing of the four remaining unshared oxygen atoms to form a two-dimensional architecture of a puckered polyoxyanion spreading along (010). Upon cooling, $CsCoO_2$ undergoes a virtually second order phase transition at ~100 K leading to a systematic dovetail twin (*C*2/*c*). The magnetic susceptibilities show the dominance of antiferromagnetic interactions with a remarkably high Néel temperature of 430 K indicating a very strong antiferromagnetic superexchange between the Co^{3+} ions. The spin-exchange for $CsCoO_2$ can be addressed as a set of strongly antiferromagnetically coupled quasi-one-dimensional chains, which are weakly coupled to neighboring chains by ferromagnetic interaction.

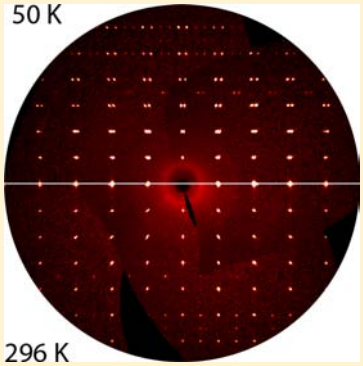

INTRODUCTION

Oxometalates of 3d transition elements feature a rich diversity of interesting physical properties, which often give rise to quite beneficial functionalities. This holds true for oxocobaltates in particular, where well performing thermoelectrics ($NaCo_2O_4$, $Ca_3Co_4O_9$),[1] battery materials ($LiCoO_2$),[2] or superconductors ($Na_xCoO_2{\cdot}yH_2O$)[3] have been encountered. From the perspective of basic research substantial progress has been achieved in recent times. In addition to the historically dominating oxidation states of 2+ and 3+, the exotically low valence state of 1+ has been realized for cobalt and its congeners iron and nickel.[4] Furthermore, a series of well-defined oxocobaltates(IV) has become available.[5]

In retrospect, the magnetic behavior of Co^{3+} in multinary oxides[6] appeared to be quite uniform, inasmuch as mostly the d^6 electron configuration in octahedral coordination with a low spin was encountered. Later on, residual magnetic responses were observed in several cases. This has led to the proposal of "intermediate" spin states,[6f] and now, after repeated observations, we consider Co^{3+} in tetrahedral coordination as quite common.[7,5f,g]

In this report we present $CsCoO_2$ as another example for cobalt(III) in tetrahedral coordination. For the most part the ABO_2 family of compounds is dominated by rock salt type order variants, β-$LiFeO_2$ and α-$NaFeO_2$ type of structures, by zinc blende type of arrangements, e.g., $LiGaO_2$, and stuffed cristobalite derived structures.[8] Less frequently, the β-$RbScO_2$ type is encountered.[9] Interestingly, the respective cobaltates(III) display a conspicuous variety of partly singular for oxides structures, like $KCoO_2$ with cobalt in 5-fold square pyramidal coordination.[7a] A second polymorph of $KCoO_2$,[7b] and $RbCoO_2$,[7a] forms stuffed cristobalite types of structure, while the structure of $CsCoO_2$ was unknown so far. $CsCoO_2$, as now synthesized along the azide/nitrate route,[5g,10] represents a crystal structure novel for oxides that is based on a two dimensionally infinite polyoxoanion of corner and edge sharing tetrahedra. This special connectivity gives rise to a strongly exchange coupled magnetic ground state.

EXPERIMENTAL SECTION

Material Synthesis. $CsCoO_2$ has been prepared along the azide/nitrate route[5g,10] as a reddish black microcrystalline powder. Starting materials were CsN_3, $CsNO_3$ (Sigma-Aldrich, 99%), and Co_3O_4. The latter was prepared by decomposing $Co(C_2O_4){\cdot}2H_2O$ (Johnson Matthey, 99%) in a flow of oxygen at 623 K for 20 h, whereas the CsN_3 was synthesized from aqueous HN_3 and cesium carbonate.[11]

The starting materials were mixed in the ratio required according to eq 1, ground in a ball mill, pressed in pellets (⌀ 13 mm) under 10^5 N, dried under vacuum (10^{-3} mbar) at 423 K overnight, and placed under argon in a closed steel vessel,[5g,10] provided with a silver inlay. In a flow of dry argon the following temperature profile was applied: 298→533 K (100 K/h), 533→653 K (5 K/h), 653→833 K (20 K/h), with subsequent annealing for 60 h at 833 K.

$$14CsN_3 + 4CsNO_3 + 6Co_3O_4 = 18CsCoO_2 + 23N_2 \quad (1)$$

Hazards. ***Caution!*** *The heating profile as stated above must be followed strictly; when heating at a higher speed the containers may blow up!*

Alternatively, $CsCoO_2$ has also been synthesized from the respective binary oxides employing the classical ceramic method. Stoichiometric amounts of starting materials (Cs_2O, CsO_2, and Co_3O_4) were thoroughly mixed, placed in a silver crucible, sealed under argon in a quartz tube, and finally thermally treated at 923 K for 20 h. The two

Received: July 26, 2012
Published: October 31, 2012

   dx.doi.org/10.1021/ic301637w | *Inorg. Chem.* 2012, 51, 12336−12342

alternative routes yield samples of the same quality. In contrast to the ceramic method, by employing the azide/nitrate route, the high reactivity of respective binary oxides forming "*in situ*", together with the thermodynamic driving force and favorable kinetic conditions simplify the preparative work.

The obtained single phase $CsCoO_2$ powders, being extremely sensitive to humid air, were sealed in glass ampules under argon atmosphere, and all following manipulations with these substances were performed in inert atmospheres of purified argon.

Single Crystal X-ray Structure Determination. Single crystals of $CsCoO_2$ of sufficient size were obtained after 400 h of annealing of a powder sample at 873 K, in silver crucibles, enclosed in quartz glass ampules under dried Ar. A suitable crystal of approximate size 0.18 × 0.12 × 0.08 mm^3 was singled out and mounted in a sealed glass capillary in a drybox under an argon atmosphere (O_2, H_2O < 0.1 ppm, M. Braun GmbH, Garching, Germany).

Ambient temperature single crystal diffraction data were collected on a three circle diffractometer (Bruker AXS, Karlsruhe, Germany) equipped with a SMART-CCD (APEX I), at 296 K. The collection and reduction of data were carried out with the Bruker Suite software package.[12] Intensities were corrected for absorption effects applying a multiscan method with SADABS.[13] The structure was solved by direct methods and refined by full matrix least-squares fitting with the SHELXTL software package.[14]

As we found out that $CsCoO_2$ undergoes a phase transition upon cooling, another set of single crystal intensities was collected at 50 K using a second crystal of 0.12 × 0.04 × 0.03 mm^3 in size [Smart APEX-II diffractometer, equipped with the N-Helix low temperature device, Oxford Cryosystems Ltd., Oxford, United Kingdom (28−300 K)].[15] It turned out that systematic twinning occurs after phase transition (dovetail twin for the monoclinic system), and the twin-law [−100, 0−10, 001] had to be applied during data reduction. Absorption correction was performed with TWINABS.[16]

Both diffractometers used Mo Kα radiation (λ = 0.710 73 Å). Details of crystallographic data and data collection are given in Table 1, and atomic coordinates and displacement parameters can be obtained from Supporting Information (Table S1−S4).

The X-ray investigation on powder samples of cesium oxocobaltate was performed using a D8-advance laboratory diffractometer (Bruker AXS, Karlsruhe, Germany) with Mo Kα_1 radiation (λ = 0.709 300 Å). Diffraction patterns were collected at room temperature in the 2θ range 4.0−55.0° with a total sample exposure time of 20 h sealed in a 0.3 mm quartz capillary (Hilgenberg), kept rotating during data collection for better particle statistics. Structural refinements have been performed with the TOPAS program[18] (version 4.1, Bruker AXS) by employing the Rietveld refinement technique.[19] As starting parameters in the structure refinement, the atomic coordinates found in the single crystal X-ray investigation were used. No extra reflections were observed compared to those calculated from atomic coordinates as determined by single-crystal structure analysis, see Figure 1, and Supporting Information Table S6.

Thermal analyses of as synthesized polycrystalline samples of $CsCoO_2$ were carried out using a DTA/TG device (STA 409, Netzsch). The sample was heated up to 1473 K at a rate of 10 K/min in a corundum crucible under dry argon.

The temperature dependence of the specific heat (C_p) of a polycrystalline sample of $CsCoO_2$ was measured between 4 and 200 K using a quasiadiabatic heat pulse method (Nernst calorimeter).[20] The powder samples (~100 mg) were encapsulated in Duran glass ampules under ~1 bar of He gas to provide sufficient thermal coupling. The glass ampules were attached with a minute amount of Apiezon vacuum grease to the sapphire sample disk platform. The heat capacity of the glass ampule, Apiezon grease, and sample holder were subtracted from total heat capacities.

The magnetic susceptibility $\chi(T)$ of polycrystalline powder samples of $CsCoO_2$ were measured in the temperature range from 2 to 700 K in magnetic fields up to 7 T using a MPMS-XL7 SQUID magnetometer (Quantum Design, 6325 Lusk Boulevard, San Diego). The moisture sensitive samples were sealed in carefully dried SUPRASIL ampules (⌀ = 3 mm), the magnetizations of which were determined in separate runs and subtracted. For the measurements above room-temperature the samples were wrapped in thin-walled gold foil in order to avoid direct contact of the samples with the glass walls. The quartz glass tubes were flushed with 1 bar He gas to provide adequate thermal contact to the cryostat. The raw data obtained was finally corrected for the temperature independent term $\chi_o = \chi_{dia} + \chi_{VV}$ which accounts for core electrons diamagnetic contribution (χ_{dia}) and

Table 1. Crystal Data, Data Collection, and Refinement Details of α- and β-$CsCoO_2$

T/K, type	296(2), β	50.0(2), α
cryst syst	orthorhombic	monoclinic
space group (No.), Z	*Cmca* (64), 8	*C*2/*c* (15), 8
lattice constants[a] /Å or deg	a = 5.9841(1)	a = 5.973(1)
	b = 12.2458(2)	b = 12.207(2)
	c = 8.2650(1)	c = 8.227(2)
		β = 91.578(3)
V /Å^3	605.66(2)	599.7(2)
$\rho_{x\text{-ray}}$/g cm^{-3}	4.910	4.959
cryst size/mm^3	0.18 × 0.12 × 0.08	0.12 × 0.04 × 0.03
diffractometer	Smart APEX I, Bruker AXS	Smart APEX II, Bruker AXS
X-ray radiation, λ /Å	0.710 73	0.710 73
abs corr	multiscan, SADABS[13]	multiscan, TWINABS[16]
2θ range /deg	6.6 ≤ 2θ ≤ 73.4	6.6 ≤ 2θ ≤ 72.9
index range	−9 ≤ h ≤ 9	−9 ≤ h ≤ 9
	−20 ≤ k ≤ 20	0 ≤ k ≤ 20
	−13 ≤ l ≤ 13	0 ≤ l ≤ 13
reflns collected	5431	8027[b]
unique reflections, R_{int}	806, 0.021	2464[b], 0.053
no. params	24	39
transm t_{max}, t_{min}	0.339, 0.147	0.623, 0.229
R1[$F^2 > 2\sigma(F^2)$]	0.0163	0.0343
wR(F^2)	0.0387	0.0926
twin volume fractions		0.513(1), 0.487
deposition no.[17]	CSD-424937	CSD-424936

[a]296 K: Lattice constants extracted from powder data. 50 K: Lattice constants from single crystal data. [b]50 K: Reflections collected contain single and composite intensities of both twin fractions. Symmetry equivalent reflections were merged after absorption correction.

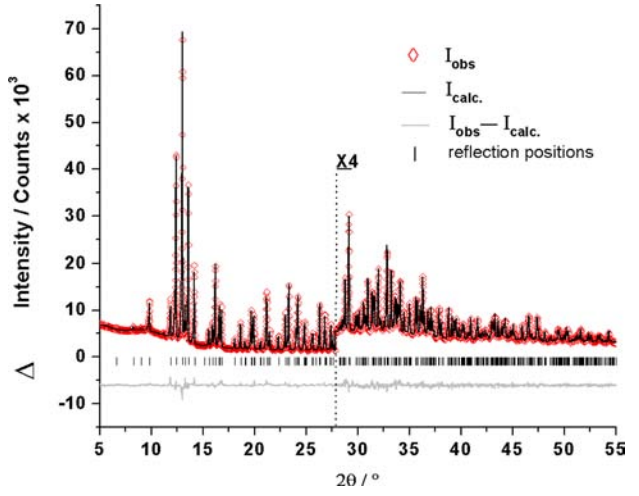

Figure 1. Scattered X-ray intensity for a polycrystalline sample of $CsCoO_2$ at T = 298 K as a function of diffraction angle 2θ (λ = 0.709 300 Å), showing the observed pattern (diamonds), the best Rietveld-fit profile (black line), reflection markers (vertical bars), and difference plot $\Delta = \mathbf{I}_{obs} - \mathbf{I}_{calc}$ (gray line) (shifted by a constant amount).

dx.doi.org/10.1021/ic301637w | *Inorg. Chem.* 2012, 51, 12336−12342

potential van Vleck paramagnetic contribution (χ_{VV}) for the Co^{3+} ion. The diamagnetic susceptibility of the core electrons in closed shells can be estimated by the incremental method using data as tabulated, e.g, by Lueken,[21] resulting in a total diamagnetic contribution of χ_{dia}= -65.25×10^{-6} cm^3/mol per formula unit. The Van Vleck paramagnetic contribution per Co^{3+} cation amounts to 100×10^{-6} cm^3/mol.

RESULTS AND DISCUSSION

New $CsCoO_2$ has been synthesized along the azide/nitrate route, and alternatively from respective mixtures of binary oxides. $CsCoO_2$ is stable up to ~1200 K, where decomposition accompanied by weight loss (Figure S2) occurs leaving behind mixtures of CoO[22] and Co_3O_4[23] as the only solid residues. Conversely, upon cooling a displacive structural phase transition is encountered with an onset at $T \sim 100$ K.

Crystal Structure. $CsCoO_2$ crystallizes in the $BaSiN_2$ type of structure,[24] with the orthorhombic space group *Cmca* (No. 64), and the lattice parameters $a = 5.9841(1)$ Å, $b = 12.2458(2)$ Å, $c = 8.2650(1)$ Å, determined from powder diffraction data (cf., Table 1). The prominent features of the structure are pairs of edge-linked CoO_4 tetrahedra to form Co_2O_6 dimers, and these units are condensed by vertex sharing of the four remaining unshared oxygen atoms to form a two-dimensional puckered polyoxyanion spreading along (010); parallel sheets are separated by cesium ions, see Figure 2.

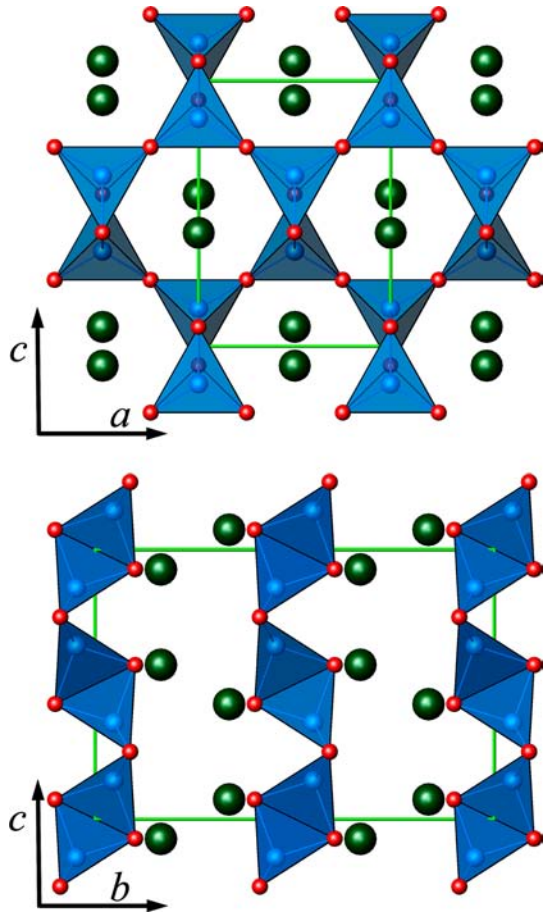

Figure 2. Projection of the crystal structure of $CsCoO_2$ (at 296 K). Top shows view along [010]. Bottom shows view along [100]. Color code: CoO_4 tetrahedra (blue), cesium (green), oxygen (red), with margins of the unit cell (green).

The Co−O bond lengths agree, on average, well with the data reported in the literature[7] and with the sum of ionic radii. The Co−O1 distances of 1.890(1), 1.896(2) Å (common edge) are substantially longer than the two Co−O2 distances of 1.808(7) Å (common vertices), cf., Table 2. Furthermore, the

Table 2. Selected Bond Distances (Å) and Angles (deg)

distance/angle	296 K	mult	50 K	mult
Co−O1	1.890(1)	1	1.895(2)	1
Co−O1	1.896(2)	1	1.899(2)	1
Co−O2	1.8077(7)	2	1.819(1)	1
Co−O3			1.814(1)	1
Co−Co	2.6264(7)	1	2.6125(8)	1
Cs−O1	3.035(2)	1	3.015(2)	1
Cs−O1	3.0945(5)	2	3.084(3)	1
Cs−O1	3.123(2)	1	3.091(3)	1
Cs−O1			3.105(2)	1
Cs−O2	3.2037(7)	2	3.166(1)	1
Cs−O3			3.175(1)	1
O1−Co−O1	92.14(8)	1	93.0(1)	1
O1−Co−O2	111.64(5)	2	112.9(1)	1
O1−Co−O2			109.8(1)	1
O1−Co−O2	114.15(7)	2	112.5(1)	1
O1−Co−O2			116.7(1)	1
O2−Co−O2	111.70(6)	1		
O2−Co−O3			110.90(7)	1
Co−O1−Co	87.85(8)	1	87.0(1)	1
Co−O2−Co	148.5(2)	1	140.5(2)	1
Co−O3−O3			153.0(3)	1

O2−Co−O2 angle of 111.70(6)° is close to the ideal tetrahedral angle (109.5°), whereas the O1−Co−O1 angle associated with the shared edge is greatly reduced to 92.14(8)°. Detailed inspection of the Co−O distances and respective angles reveals a substantial distortion in the structure, as a consequence of repulsion between Co atoms separated by the shared tetrahedral edges. The scenario can be easily rationalized in terms of the different functionalities of the oxygen atoms involved. As a rule, edges shared by two polyhedra are contracted, while the centering cations repel each other; accordingly, the corresponding angle O1−Co−O1 (92.14°) is also contracted, cf., Table 2 and Figure S1. The cesium atoms are coordinated by six oxygen atoms in the form of a strongly distorted pentagonal pyramid with Cs−O distances varying from 3.035(2) to 3.2037(7) Å, which is in the expected range.[5]

MAPLE calculations[25] were performed for $CsCoO_2$ as a means of checking the plausibility of this new structure. The calculated value (9961 kJ/mol) for $CsCoO_2$ and the sums of the calculated partial Madelung energies derived from respective binary oxides (9887 kJ/mol) agree well with a deviation as low as 0.7%, which is well within the permissible limit thereby reflecting the high quality of the structure refinements (cf., Table S5).

Thermal analysis and magnetic susceptibility measurements indicated a virtually second order phase transition at ~100 K. The structural phase transition was monitored independently by cooling down a single crystal in situ on a diffractometer. The structure of the transformation twin of the low temperature form (α-$CsCoO_2$) was solved and refined using the intensity data of both twin domains (cf., Figure 3a). Its space group *C*2/*c* (Table 1) is a maximal nonisomorphic subgroup of the space group *Cmca* (type *translationengleich* of index 2), of β-$CsCoO_2$.

dx.doi.org/10.1021/ic301637w | *Inorg. Chem.* 2012, 51, 12336−12342

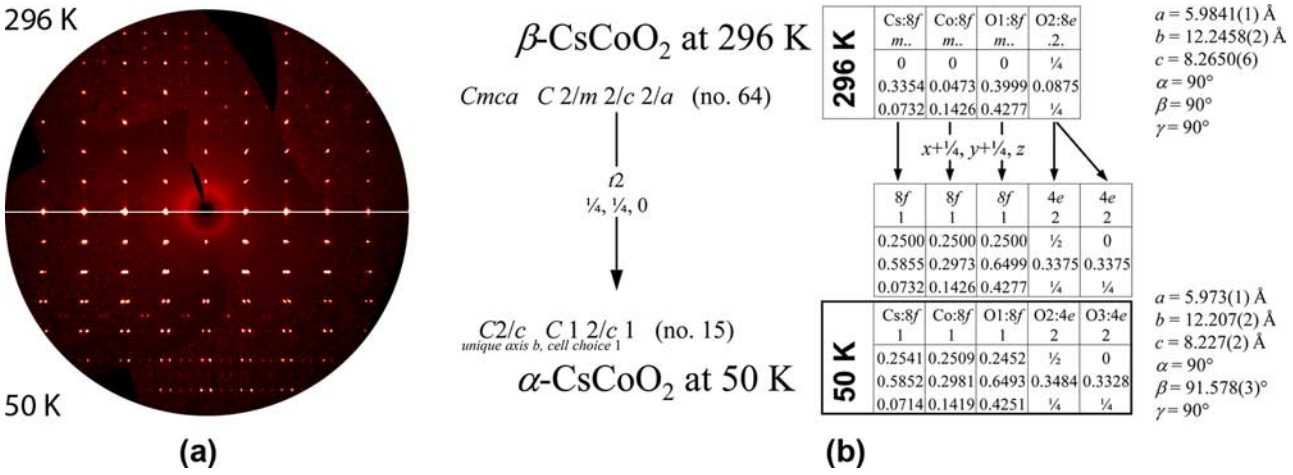

Figure 3. (a) Reciprocal layer (*h*0*l*) for the orthorhombic room temperature phase of $CsCoO_2$, at T = 296 K with lower inset showing splitting of peaks (due to twinning) at T = 50 K attributed to monoclinic distortion. (b) Group-subgroup relation between the high temperature (296 K) and low temperature (50 K) structures of $CsCoO_2$. The boxes contain: element, Wykoff symbol, site symmetry, and atomic coordinates x, y, z. Lattice parameters are specified in addition.

Figure 3b shows the group−subgroup relation, including all site transformations for both modifications.[26] A comparison between the atomic coordinates indicates that the major structural changes are reflected by the splitting of the former 8*e* site (296 K) of O2 in 2 × 4*e* sites O2 and O3 (50 K), and splitting of y = 0.3375 to y = 0.3484 and 0.3328, respectively (Figure 3). These shifts, together with the monoclinic angle of 91.578°, result in a significant tilting of the Co_2O_6 units (edge sharing tetrahedra), which is most distinctly seen by the Co−O−Co angles of the oxygen atoms (O2, O3) mediating corner sharing of tetrahedra. The Co−O2−Co bonding angle of 148.5° in β-$CsCoO_2$ splits into 140.5° (Co−O2−Co) and 153.0° (Co−O3−Co) upon cooling (Table 2). The distortion in α-$CsCoO_2$ allows for a more dense packing of the structure, although the Co−O distances are slightly larger as compared to the β-form (Table 2).

Thermal Analysis and Magnetic Characterization. Figure 4 displays the heat capacity, C_p/T, versus temperature in a semilogarithmic plot. The insert highlights the temperature range around 100 K. The heat capacity grows steadily and has not yet saturated at the Petit−Dulong value of 12 × R, where R is the molar gas constant. At 200 K the heat capacity has a value of 74 J/(mol K). A sluggish smeared bump is seen in the temperature centered near 85 K and extends over a temperature range ∼± 10 K indicating a considerably smeared phase transition with little entropy involved. The change of entropy amounts to ∼0.1 to 0.2 J/(mol K). A λ-type anomaly or signatures of a thermal hysteresis were not found in the heat capacity measurements.

In order to construct a model for the spin interactions in $CsCoO_2$, the magnetic properties of $CsCoO_2$ have been measured in the temperature range from 2 to 700 K in magnetic fields up to 7 T as displayed in Figure 5.

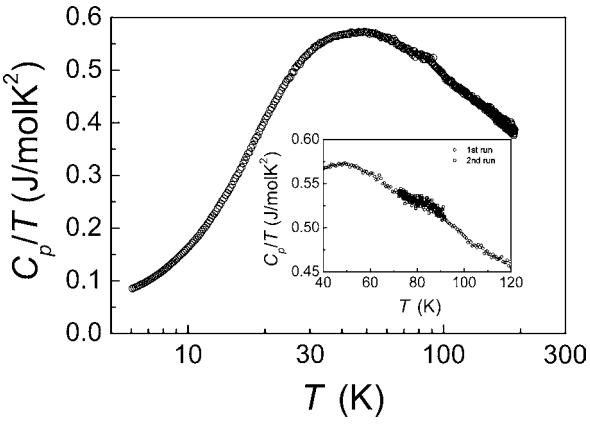

Figure 4. Heat capacity of a polycrystalline sample of $CsCoO_2$ versus temperature. The main frame shows C_p/T in a semilogarithmic plot; the insert highlights the temperature range around 80 K.

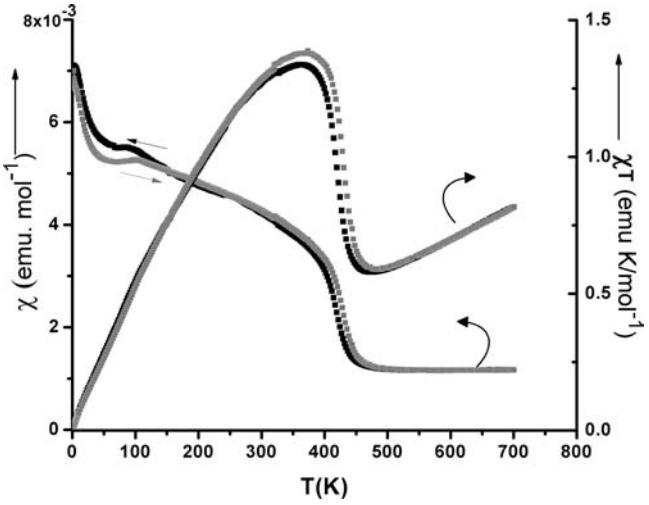

Figure 5. Temperature dependence of magnetic susceptibility for $CsCoO_2$ represented as χ vs T and χT vs T. The heating curve (gray squares) has been measured after the sample has been zero-field cooled (black squares) to 2 K.

Magnetic susceptibility and heat capacity data indicate long-range antiferromagnetic ordering below ∼430 K and an additional phase transition at ∼100 K. Both magnetic as well as structural phase transitions exhibit a thermal hysteresis. If the magnetic susceptibility is measured while cooling the sample, the anomalies appear systematically lower in temperature than the anomalies measured with increasing temperature. The 430

dx.doi.org/10.1021/ic301637w | Inorg. Chem. 2012, 51, 12336−12342

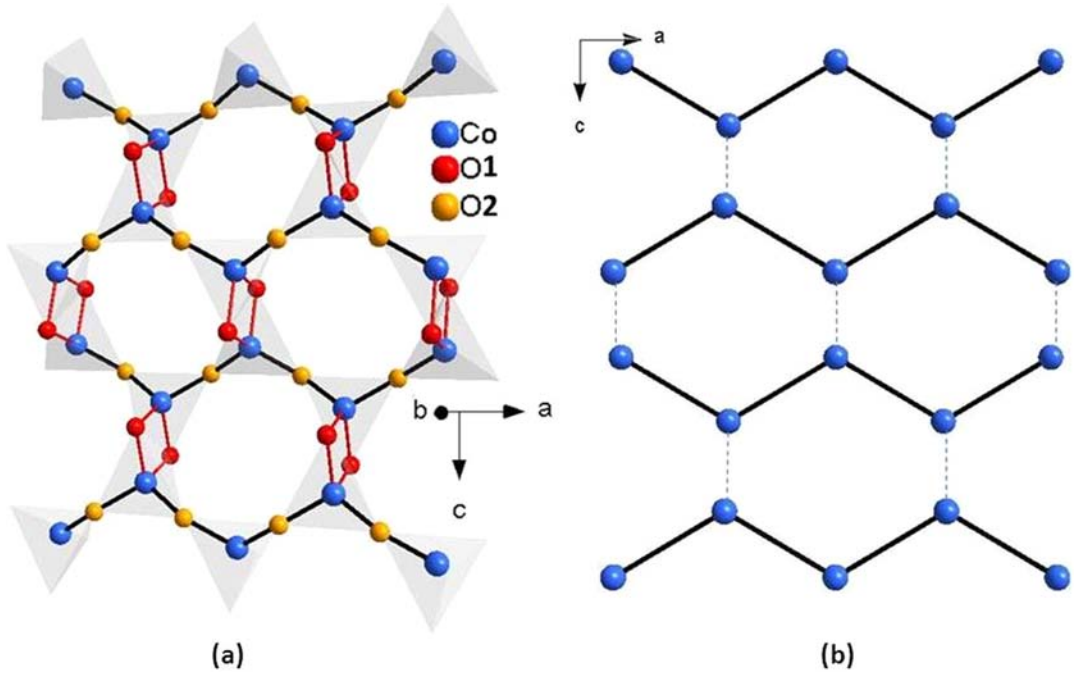

Figure 6. Crystal structure of $CsCoO_2$ emphasizing spin exchange paths. (a) The black solid lines connect Co atoms along the crystallographic *a* direction via O2 atoms. The Co−O2−Co bonding angle amounts to 148.4°. O1 atoms connect the chains with a Co−Co bonding angle of 87.9°. (b) Spin-exchange model suggested for $CsCoO_2$.

Table 3. Geometrical and Magnetic Parameters of Co(III)−O−Co(III) Spin Exchange Paths in Some Selected Oxocobaltates

compd	type	Co−Co distance/Å	Co−O−Co angle/deg	J_{FM} /cm^{-1}	*g*	T_c/T_N/K	ref
$Na_{10}Co_4O_{10}$	$[Co_4O_{10}]^{10-}$ tetramer	2.78	91.6		2.15	37	7f,g
$Na_6Co_2O_6$	$[Co_2O_6]^{6-}$ dimers	2.875	93.94	3.5	2.19	30	7h
$CsCoO_2$	$[CoO_2]^{1-}$ chains	2.626	87.85			430	this study

K phase transition is downshifted by about 10 K and the 100 K phase transition by about 20 K. Above 450 K the magnetic susceptibility is temperature independent; a Curie−Weiss law type behavior is not seen most likely due to extended short-range ordering effects enhanced by the rather large measuring field. In view of the structural and magnetic similarities with $Na_{10}Co_4O_{10}$[7f,g] showing a collinear antiferromagnetic spin structure, we propose a spin-exchange model for $CsCoO_2$ shown in Figure 6. The remarkably high Néel temperature of 430 K in $CsCoO_2$ points to a very strong antiferromagnetic superexchange between the Co^{3+} cations[27] in line with Goodeneough−Kanamori rules.[28]

The development of the weak spontaneous polarization below the Néel temperature points to a slight canting of the moments. In order to understand the magnetic properties we inspected possible spin-exchange paths in the crystal structure of $CsCoO_2$. Figure 6a displays a section of the crystal structure of $CsCoO_2$. It reveals that the Co atoms are connected via O2 atoms to form chains running along the crystallographic *a* direction. The bonding angle, Co−O—Co, amounts to 148.4°. This arrangement may be expected to support strong antiferromagnetic spin-exchange interaction. Such chains are connected via O1 atoms which enclose a bonding angle of 87.9° with the two adjacent Co atoms (cf., Figure S1).

Spin-exchange via such oxygen bonds with bonding angle close to 90° may be expected to be very weak and possibly ferromagnetic.[28] In fact, the analysis of the magnetic susceptibility of related Co^{3+} oxocobaltates with Co−O−Co bonding angles close to 90° and Co−Co distances similar to those in $CsCoO_2$ (see Table 3) reveals ordering temperatures which are by at least an order of magnitude lower than that of $CsCoO_2$.

We therefore ascribe the strong spin-exchange interaction in $CsCoO_2$ to exchange coupling of the Co atoms via the O2 atoms which effectively establishes a Co−O−Co chain along *a*. Here the Co−O−Co bonding angle is of the order of ∼150° and may be expected to support strong antiferromagnetic superexchange. Within this model, $CsCoO_2$ may be described as a set of strongly antiferromagnetically coupled quasi-one-dimensional chains which are weakly coupled to neighboring chains by a ferromagnetic interchain interaction (see Figure 6b).

The magnetic susceptibility of antiferromagnetically coupled linear chains is characterized by an extended short-range ordering bulge with its maximum at a temperature which is proportional to the intrachain spin-exchange interaction. In case of a very strong intrachain antiferromagnetic coupling the susceptibility at temperatures below the maximum slowly decreases with decreasing temperature.[29] Within the proposed scenario of weakly ferromagnetically coupled antiferromagnetic chains the largely temperature independent magnetic susceptibility seen for $CsCoO_2$ between 700 K and the Néel temperature can be understood as due to a superposition of such a weakly decreasing linear-chain susceptibility and the ferromagnetic correlations between the chains which finally lead to long-range ordering and the observed weak spontaneous magnetic polarization below the Néel temperature.

dx.doi.org/10.1021/ic301637w | *Inorg. Chem.* 2012, 51, 12336−12342

CONCLUSIONS

We report a novel oxide structure type, realized for $CsCoO_2$, featuring a unique polyoxocobaltate(III) anion based on a two-dimensional architecture of interconnected tetrahedra, undergoing a virtually second order phase transition at ∼100 K. The magnetic susceptibilities show the dominance of antiferromagnetic interactions with a remarkably high Néel temperature of 430 K indicating a very strong antiferromagnetic superexchange between the Co^{3+} ions along quasi-one-dimensional chains, which are weakly coupled to neighboring chains by a ferromagnetic interchain interaction. To corroborate and to get further insight into the magnetic behavior of the title compound, in particular, to comprehend the interplay of intra- and inter chain exchange interactions, the neutron scattering experiments are underway.

ASSOCIATED CONTENT

Supporting Information

Additional tables and figures. This material is available free of charge via the Internet at http://pubs.acs.org.

AUTHOR INFORMATION

Corresponding Author

*E-mail: M.Jansen@fkf.mpg.de. Phone: 0049-711-689 1500. Fax: 0049-711-689 1502.

Notes

The authors declare no competing financial interest.

ACKNOWLEDGMENTS

The authors would like to express thanks to E. Brücher for performing the magnetic measurements. We thank Claus Muehle for his technical support throughout the experimental work.

REFERENCES

(1) (a) Jansen, M.; Hoppe, R. *Z. Anorg. Allg. Chem.* **1974**, *408*, 104. (b) Terasaki, I.; Sasago, Y.; Uchinokura, K. *Phys. Rev. B* **1997**, *56*, 12685. (c) Maignan, A.; Hebert, S.; Pi, L.; Pelloquin, D.; Martin, C.; Michel, C.; Hervieu, M.; Raveau, B. *Cryst. Eng.* **2002**, *5*, 365. (d) Masset, A. C.; Michel, C.; Maignan, A.; Hervieu, M.; Toulemonde, O.; Studer, F.; Raveau, B.; Hejtmanek, J. *Phys. Rev. B* **2000**, *62*, 166.

(2) (a) Bongers, P. F. *Ph.D. Thesis*. University of Leiden, Leiden, The Netherlands, 1957. (b) Mizushima, K.; Jones, P. C.; Wiseman, P. J.; Goodenough, J. B. *Mater. Res. Bull.* **1980**, *15*, 783.

(3) (a) Takada, K.; Sakurai, H.; Takayama-Muromachi, E.; Dilanian, R. A.; Sasaki, T. *Nature* **2003**, *422*, 53. (b) Schaak, R. E.; Klimczuk, T.; Foo, M. L.; Cava, R. J. *Nature* **2003**, *424*, 527. (c) Chou, F. C.; Cho, J. H.; Lee, P. A.; Abel, E. T.; Matan, K.; Lee, Y. S. *Phys. Rev. Lett.* **2004**, *92*, 157004. (d) Fujimoto, T.; Zheng, G.-q.; Kitaoka, Y.; Meng, R. L.; Cmaidalka, J.; Chu, C. W. *Phys. Rev. Lett.* **2004**, *92*, 047004.

(4) (a) Burow, W.; Birx, J.; Bernhardt, F.; Hoppe, R. *Z. Anorg. Allg. Chem.* **1993**, *619*, 923. (b) Bernhardt, F.; Hoppe, R.; Kremer, R. K. *Z. Anorg. Allg. Chem.* **1994**, *620*, 187. (c) Sofin, M.; Jansen, M. *Z. Anorg. Allg. Chem.* **2001**, *627*, 2115.

(5) (a) Jansen, M.; Hoppe, R. *Z. Anorg. Allg. Chem.* **1974**, *408*, 75. (b) Jansen, M. *Z. Anorg. Allg. Chem.* **1975**, *417*, 35. (c) Jansen, M.; Hoppe, R. *Z. Anorg. Allg. Chem.* **1973**, *398*, 54. (d) Jansen, M.; Hoppe, R. *Naturwissenschaften* **1973**, *60*, 104. (e) Jansen, M.; Hoppe, R. *Z. Anorg. Allg. Chem.* **1974**, *409*, 152. (f) Müller-Buschbaum, Hk. *Z. Anorg. Allg. Chem.* **2012**, *638*, 1. (g) Jansen, M. *Z. Anorg. Allg. Chem.* **2012**, *638*, 1910.

(6) (a) Weidenkaff, A.; Aguirre, M. H.; Bocher, L.; Trottmann, M.; Robert, R. *The Development of Thermoelectric Oxides with Perovskite-Type Structures for Alternative Energy Technologies*; Advances in Electronic Ceramics: Ceramic Engineering and Science Proceedings; John Wiley & Sons, Inc.: New York, 2009; Vol. *28*(8), Chapter 17, DOI: 10.1002/9780470339817.ch17. (b) Weidenkaff, A.; Aguirre, M. H.; Bocher, L.; Trottmann, M.; Tomes, P.; Robert, R. *J. Korean Ceram. Soc.* **2010**, *47*, 47. (c) Conder, K.; Pomjakushina, E.; Soldatov, A.; Mitberg, E. *Mater. Res. Bull.* **2005**, *40*, 257. (d) Maignan, A.; Martin, C.; Pelloquin, D.; Nguyen, N.; Raveau, B. *J. Solid State Chem.* **1999**, *142*, 247. (e) Koshibae, W.; Tsutsui, K.; Maekawa, S. *Phys. Rev. B* **2000**, *62*, 6869. (f) Bezdicka, P.; Wattiaux, A.; Grenier, J. C.; Pouchard, M.; Hagenmuller, P. *Z. Anorg. Allg. Chem.* **1993**, *619*, 7.

(7) (a) Jansen, M.; Hoppe, R. *Z. Anorg. Allg. Chem.* **1975**, *417*, 31. (b) Delmas, C.; Fouassier, C.; Hagenmuller, P. *J. Solid State Chem.* **1975**, *13*, 165. (c) Burow, W.; Hoppe, R. *Naturwissenschaften* **1980**, *67*, 192. (d) Birx, J.; Hoppe, R. *Z. Anorg. Allg. Chem.* **1991**, *597*, 19. (e) Baker, L. C. W.; McCutcheon, T. P. *J. Am. Chem. Soc.* **1956**, *78*, 4503. (f) Sofin, M.; Güdel, H.-U.; Bircher, R.; Peters, E.-M.; Jansen, M. *Angew. Chem.* **2003**, *115*, 3651; *Angew. Chem., Int. Ed.* **2003**, *42*, 3527. (g) Stüsser, N.; Sofin, M.; Bircher, R.; Güdel, H.-U.; Jansen, M. *Chem.—Eur. J.* **2006**, *12*, 5452. (h) Sofin, M.; Peters, E.-M.; Jansen, M. *J. Solid State Chem.* **2004**, *177*, 2550.

(8) (a) O'Keefe, M.; Hyde, B. G. *Acta Crystallogr., Sect. B* **1976**, *32*, 2923. (b) Ali, N. Z.; Nuss, J.; Sheptyakov, D.; Jansen, M. *J. Solid State Chem.* **2010**, *183*, 752.

(9) (a) Hoppe, R.; Sabrowsky, H. *Z. Anorg. Allg. Chem.* **1965**, *339*, 144. (b) Wiench, H.; Brachtel, G.; Hoppe, R. *Z. Anorg. Allg. Chem.* **1977**, *436*, 169.

(10) (a) Trinschek, D.; Jansen, M. *Angew. Chem., Int. Ed.* **1999**, *38*, 133. (b) Sofin, M.; Peters, E.-M.; Jansen, M. *Z. Anorg. Allg. Chem.* **2002**, *628*, 2697.

(11) (a) Brauer, G. *Handbuch der Praparativen Anorganischen Chemie*, 1st ed.; F. Enke Verlag: Stuttgart, 1975; p 457. (b) Fair, H. D.; Walker, R. F. *Energetic Materials, Physics and Chemistry of Inorganic Azides*; Plenium Press: New York, 1977; Vol. *1*, pp 30−38.

(12) *Bruker Suite, version 2008/3*; Bruker AXS Inc.: Madison, WI, 2008.

(13) Sheldrick, G. M. *SADABS—Bruker AXS Area Detector Scaling and Absorption, version 2008/1*; University of Göttingen: Göttingen, Germany, 2008.

(14) Sheldrick, G. M. *Acta Crystallogr., Sect. A* **2008**, *64*, 112.

(15) Cakmak, G.; Nuss, J.; Jansen, M. *Z. Anorg. Allg. Chem.* **2009**, *635*, 631.

(16) Sheldrick, G. M. *TWINABS—Bruker AXS Scaling for Twinned Crystals, version 2008/4*; University of Göttingen: Göttingen, Germany, 2008.

(17) Further details of the crystal structure investigations may be obtained from the Fachinformationszentrum Karlsruhe, 76344 Eggenstein-Leopoldshafen, Germany (fax (+49)7247-808-666, e-mail crysdata(at)fiz-karlsruhe.de) on quoting the depository number CSD-424936 and CSD-424937.

(18) Coelho, A. A. *J. Appl. Crystallogr.* **2003**, *36*, 86.

(19) Rietveld, H. M. *J. Appl. Crystallogr.* **1969**, *2*, 65.

(20) Schnelle, W.; Gmelin, E. *Thermochim. Acta* **2002**, *391*, 41.

(21) Lueken, H. *Magnetochemie*; Teubner: Leipzig, 1999.

(22) Natta, G.; Reina, A. *An. Fis. Quim.* **1926**, *24*, 611.

(23) Natta, G.; Schmidt, F. *Gazz. Chim. Ital.* **1928**, *58*, 419.

(24) Gál, Z. A.; Mallinson, P. M.; Orchard, H. J.; Clarke, S. J. *Inorg. Chem.* **2004**, *43*, 3998.

(25) (a) Hoppe, R. *Angew. Chem., Int. Ed. Engl.* **1966**, *5*, 95. (b) Hoppe, R. *Angew. Chem., Int. Ed. Engl.* **1970**, *9*, 25. (c) Huebenthal, R. *MAPLE, Program for the Calculation of the Madelung Part of Lattice Energy*; University of Giessen: Giessen, Germany, 1993.

(26) (a) Mueller, U. *Symmetrie Beziehungen Zwischen Verwandten Kristallstrukturen*; Vieweg+Teubner: Leipzig, 2012. (b) Wondratschek, H.; Müller, U. *International Tables for Crystallography*; Springer: Dordrecht, The Netherlands, 2008; Vol. *A1*. (c) Müller, U. *Z. Anorg. Allg. Chem.* **2004**, *630*, 1519. (d) Baernighausen, H. *MATCH* **1980**, *9*, 139.

(27) (a) Sullivan, E.; Hadermann, J.; Greaves, C. *J. Solid State Chem.* **2011**, *184*, 649. (b) Takeda, T.; Yamaguchi, Y.; Watanabe, H. *J. Phys. Soc. Jpn.* **1972**, *33*, 970. (c) Muñoz, A.; de La Calle, C.; Alonso, J. A.;

Botta, P. M.; Pardo, V.; Baldomir, D.; Rivas, J. *Phys. Rev. B* **2008**, *78*, 054404.
(28) (a) Goodenough, J. B. *Magnetism and the Chemical Bond*; Interscience: New York, 1963. (b) Kanamori, J. *J. Phys. Chem. Solids* **1959**, *10*, 87. (c) Oles, A. M.; Horsch, P.; Feiner, L. F.; Khaliulin, G. *Phys. Rev. Lett.* **2006**, *96*, 147205−1. (d) de Jongh, L. J.; Miedema, A. R. *Adv. Phys.* **2001**, *50* (8), 947.
(29) Law, J. M.; Hoch, C.; Glaum, R.; Heinmaa, I.; Stern, R.; Kang, J.; Lee, C.; Whangbo, M.-H.; Kremer, R. K. *Phys. Rev. B* **2011**, *83*, 180414.